Temperature of Dy Nuclei Excited to 40–150 MeV*

JOHN M. ALEXANDER† AND J. B. NATOWITZ‡

Department of Chemistry, State University of New York, Stony Brook, New York 11790

(Received 16 June 1969)

From the systematics of cross sections and neutron energies for (HI, xn) reactions, the average energy of the first emitted neutron has been obtained. These average energies reflect the nuclear temperature or level-density parameter. Average photon energies are also obtained and compared to calculated values of the lowest-lying levels for each spin. Reactions are considered which involve the emission of 3–11 neutrons from compound systems of 40–150 MeV and average spin 15–80. New experimental data are presented for the reactions $Nd^{148}(C^{12}, 5n)Dy^{155}$, $Nd^{150}(C^{12}, 5n)Dy^{157}$, and $Nd^{150}(C^{12}, 7n)Dy^{155}$.

I. INTRODUCTION

In a series of papers we have presented extensive experimental data on reactions of heavy ions (HI) with medium-weight nuclei (Pr^{141}, Nd^{142}, etc.).[1–5] Most of the data have been obtained by observation of the residual nuclei Dy^{149}, Dy^{150}, or Dy^{151} formed by reactions in which only neutrons and γ rays were emitted. Average values of the total energy of the photons T_γ have been determined.[2] In this work and in that by Gilat and Pape,[6] new measurements of T_n and T_γ are reported for several reactions involving significantly smaller angular momenta than those studied previously. The motivation for this work is to provide a body of data from which the statistical properties of highly excited nuclei can be obtained. These systems were particularly attractive for several reasons: (a) Recoil range data indicated that the neutron emission was essentially symmetric about 90° in the center-of-mass system,[1,4] i.e., complete deposition of energy and momentum into the transition nucleus. (b) Neutron emission is the dominant mode of decay, so that "spin fractionation" by fission or charged-particle emission is minimal.[3] (c) Observation of the intensity of α radiation from the products leads to measurements with good precision.

Any study of nuclei excited to high energies (40–150 MeV in these systems) must face the problems of multiple-particle emission. Measurements inevitably involve detection of some particle or nuclide which could have been produced by a variety of reaction paths. Calculations involve sums of differential cross sections over the various paths.[7] These complex sums can be performed, and comparison to experimental data provides the basis for the statistical description of highly excited nuclei. However, it is particularly enlightening if a measurement is made such that the inherent averaging and summing focuses predominantly on one feature of the statistical model. Such measurements might be the average kinetic energy of the first neutron or the total photon energy emitted from a nucleus of known excitation energy and angular momentum. Evaporation theory indicates that the neutron energy would mainly reflect the nuclear temperature or a parameter, while the photon energy would mainly reflect the "yrast levels" or energy of the lowest-lying states for a particular spin.[7–11]

It has not been possible to produce or to separate nuclei of specific spin, and it has not been possible to sort out the particles or photons emitted first or last in an evapoaration chain. However, it is possible to use systematic data from similar (HI, xn) reactions to unfold the average energy of the first emitted neutron. Similarly, one can obtain the average total photon energy. These average energies do not arise from nuclei of one particular angular momentum, but from that population distribution generated by the collision of a particular projectile with a particular target ($Pr^{141}+C^{12}$, $Nd^{142}+O^{16}$, etc.). The average angular momentum for such a collection can be estimated by optical-model calculations. We will present average first neutron energies which reflect the average nuclear temperature for a collection of nuclei with known average energy. Similarly, we will present average total photon energies which are closely related to the yrast levels. This analysis is an extension of that previously reported.[3] It rests on a systematic extrapolation of experimental data on T_γ for various (HI, xn) reactions. We present here some new experimental results which give T_γ for several (C^{12}, xn) reactions leading to Dy^{155} and Dy^{157}.

* Work supported by the U. S. Atomic Energy Commission.

† Alfred P. Sloan Fellow.

‡ Present address: Department of Chemistry, Texas A & M University, College Station, Tex.

[1] J. M. Alexander and D. H. Sisson, Phys. Rev. **128**, 2288 (1962).

[2] G. N. Simonoff and J. M. Alexander, Phys. Rev. **133**, B104 (1964).

[3] J. M. Alexander and G. N. Simonoff, Phys. Rev. **133**, B93 (1964).

[4] J. M. Alexander, J. Gilat, and D. H. Sisson, Phys. Rev. **136**, B1289 (1964).

[5] J. M. Alexander and G. N. Simonoff, Phys. Rev. **162**, 952 (1967).

[6] J. Gilat and A. Pape (unpublished).

[7] T. D. Thomas, Ann. Rev. Nucl. Sci. **18**, 343 (1968).

[8] J. R. Grover and J. Gilat, Phys. Rev. **157**, 802 (1967).

[9] J. R. Grover and J. Gilat, Phys. Rev. **157**, 814 (1967).

[10] J. R. Grover and J. Gilat, Phys. Rev. **157**, 823 (1967).

[11] J. R. Grover, Phys. Rev. **157**, 832 (1967).

Gilat and Pape also report some new T_γ values for (He^4, xn) reactions leading to Dy^{150} and Dy^{151}.[6] This collection of new data provides T_γ values for several systems of relatively low average angular momenta. The comparison of new and old data indicates that T_γ, for each value of x, can be represented as a linear function of excitation energy, independent of the target-projectile combination.

In Sec. II, we describe the average energy analysis, then we present new experimental data and examine the systematics of T_γ for various reactions. Finally, we give values for the average kinetic energy of the first emitted neutron and values of $\langle T_\gamma \rangle$ for each reaction.

II. AVERAGE ENERGY ANALYSIS

In former work,[3] we defined the average excitation energy $\langle E \rangle_x$ for a certain reaction of type (HI, xn)

$$\langle E \rangle_x = \int_0^\infty (E) F_x(E) dE \Big/ \int_0^\infty F_x(E) dE, \quad (1)$$

where E denotes excitation energy and F_x is the fraction of the reactions in which no charged particle is emitted that lead to the (HI, xn) reaction. Therefore, we have

$$F_x(E) = \sigma/\sigma_R f_n \quad (2)$$

and

$$\sum_{x=0}^{x_{\max}} F_x(E) = 1. \quad (3)$$

The cross section for the (HI, xn) reaction is σ, the total reaction cross section is σ_R, and the fraction of reactions in which no charged particle is emitted is f_n. The values of σ, σ_R, and f_n are known experimentally as a function of energy, and values of $\langle E \rangle_x$ have been obtained by graphical integration.[3]

The interesting feature of the quantity $\langle E \rangle_x$ is summarized by the equation[3]

$$\langle E \rangle_x = \langle E \rangle_{x-1} + B_1 + \langle \epsilon_1 \rangle \quad (4)$$

(B_1 and ϵ_1 are the binding and kinetic energies of the first emitted neutron). If one has a series of values of $\langle E \rangle_x$ for various reactions of differing x, he can obtain the average kinetic energy of the first emitted neutron. The derivation of Eq. (4) assumed that the energy spectrum of the first emitted neutron $P(\epsilon_1)$ was essentially independent of excitation energy over the region of energies important to a particular (HI, xn) reaction. Also, the omission of angular momentum from the definition of $\langle E \rangle_x$ demanded that Eq. (4) be used for reactions with the same distribution of angular momentum.

This last requirement severely limited the usefulness of Eq. (4), because it was found that values of $\langle E \rangle_x$ were rather strongly dependent on average angular momentum. This is shown in Fig. 1 (after Ref. 3). The precision of determination of $\langle \epsilon_1 \rangle$ from the data in Fig. 1 was limited by uncertainty in the delimitation of the slope of the lines and by lack of knowledge of the average angular momentum removed by the first neutron ΔJ_1.

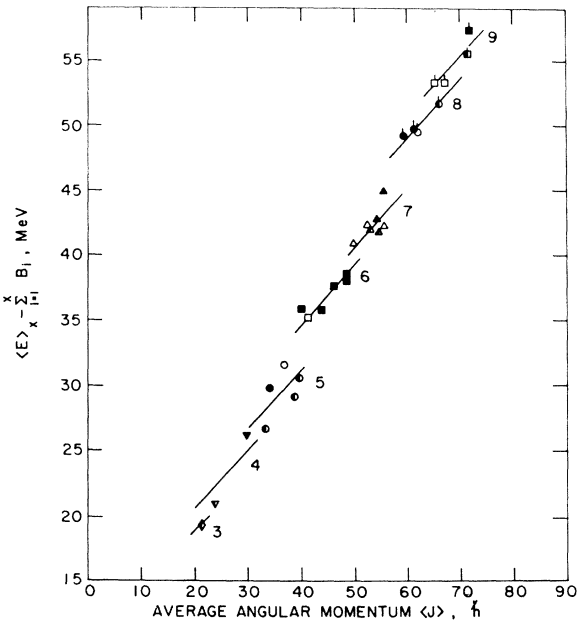

FIG. 1. Average excitation energy $\langle E \rangle_x$ minus the sum of the binding energies B_i of the neutrons as a function of the average angular momentun $\langle J \rangle$. Different symbols are used for the (HI, xn) reactions with the different x values indicated. Open points are for Dy^{149}; closed for Dy^{150}; and half-open for Dy^{151}.

The analysis just sketched can be extended by defining the average total neutron energy $\langle T_n \rangle_x$ and total photon energy $\langle T_\gamma \rangle_x$ for a certain reaction:

$$\langle T_n \rangle_x = \int_0^\infty (T_n) F_x(E) dE \Big/ \int_0^\infty F_x(E) dE \quad (5)$$

and

$$\langle T_\gamma \rangle_x = \int_0^\infty (T_\gamma) F_x(E) dE \Big/ \int_0^\infty F_x(E) dE. \quad (6)$$

The virtue of these quantities is that we can expect to focus on neutron energetics (or temperature) with $\langle T_n \rangle_x$, and on photon emission (or yrast levels) with $\langle T_\gamma \rangle_x$. In particular, we anticipate that the major source of angular momentum effects on $\langle E \rangle_x$ is through the effect of the yrast levels on $\langle T_\gamma \rangle_x$.[7] We assume that the average γ-ray energy lost with the first emitted neutron is negligible and that the total energy is a function only of the average angular momentum of the emsemble. This assumption is expressed as follows:

$$_J\langle T_\gamma \rangle_x = {}_{J-\Delta J}\langle T_\gamma \rangle_{x-1}, \quad (7)$$

where the subscripts refer to the initial average angular momentum and ΔJ_1 is the average angular momentum removed by the first neutron.

With this assumption one obtains the relationship

$$_J\langle T_n \rangle_x = {}_{J-\Delta J_1}\langle T_n \rangle_{x-1} + \langle \epsilon_1 \rangle. \quad (8)$$

TABLE I. Average angles and energies.

Bombarding energy (lab) E_b (MeV)	Corrected average angle $\langle\theta_L\rangle$ (deg)	Corrected rms angle $\langle\theta_L^2\rangle^{1/2}$ (deg)	Total available energy $E_{c.m.}+Q$ (MeV)	Average total neutron energy T_n (MeV)	Average total photon energy T_γ (MeV)
		$Nd^{148}(C^{12}, 5n)Dy^{155}$			
63.7	4.15	4.68	10.1	7.4	2.7
74.2	4.61	5.34	19.9	11.2	8.7
86.2	4.99	5.68	31.0	14.8	16.2
91.9	4.95	5.64	36.2	15.5	20.7
		$Nd^{150}(C^{12}, 5n)Dy^{157}$			
76.4	5.08	5.72	26.3	13.3	13.0
86.2	5.32	5.98	35.4	16.4	19.0
		$Nd^{150}(C^{12}, 7n)Dy^{155}$			
115.2	5.72	6.58	45.6	26.2	19.4

We expect that Eq. (8) will give more precise values of $\langle\epsilon_1\rangle$ than Eq. (4) because angular momentum dependence of $\langle T_n\rangle$ should be much less than that of $\langle E\rangle$. However, one demands knowledge of the total neutron energy T_n as a function of excitation energy. In Sec. III, we discuss the details of the systematics of T_γ and T_n and the resulting values of ${}_J\langle T_n\rangle_x$ and ${}_J\langle T_\gamma\rangle_x$.

III. SYSTEMATICS OF PHOTON AND NEUTRON ENERGIES

The evaluation of $\langle T_n\rangle_x$ and $\langle T_\gamma\rangle_x$ requires the knowledge of T_γ (or T_n) as a function of energy for each reaction. The measurements of Simonoff and Alexander[2] provide such data for nine reactions of the type (HI, xn)$Dy^{149,150,\text{or }151}$. New values of T_n are presented here for the reactions $Nd^{148}(C^{12}, 5n)Dy^{155}$, $Nd^{150}(C^{12}, 5n)Dy^{157}$, and $Nd^{150}(C^{12}, 7n)Dy^{155}$. Gilat and Pape have made similar measurements[6] for the reactions $Gd^{154}(He^4, 7n)Dy^{151}$ and $Gd^{154}(He^4, 8n)Dy^{150}$. Cross-section measurements are also reported for these reactions. Extensive cross-section measurements have been reported for 29 reactions from which values of $\langle E\rangle_x$ were extracted.[3] We now examine the 14 reactions for which T_γ data have been obtained, in an attempt to construct an empirical means of extrapolation and interpolation. Then we use the empirical systematics to divide $\langle E\rangle_x$ into $\langle T_\gamma\rangle_x$ and $\langle T_n\rangle_x$ for each of the other 29 reactions. The analysis is also extended to other

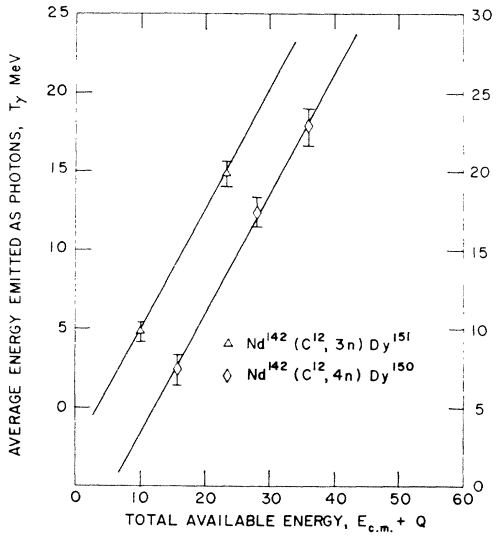

FIG. 2. Average total photon energy $T\gamma$ versus total available energy (in MeV) for (HI, $3n$) and (HI, $4n$) reactions.

TABLE II. Cross-section results.

E_b (lab) (MeV)	Relative cross section Dy^{155}	Dy^{157}
	$Nd^{150}+C^{12}\rightarrow Dy^{162}$	
60.7		618
65.6		1715
70.8		2474
74.0	7.8	2615
80.6	45.8	2230
85.0	263	1281
89.3	718	692
102.4	1647	60
114.4	822	
	$Nd^{148}+C^{12}\rightarrow Dy^{160}$	
57.4	20	552
63.4	224	229
68.6	804	51
73.6	1658	
81.4	1923	
91.7	418	
99.6	181	

TABLE III. Average total photon energies[a] for Dy nuclei.[b]

Total available energy $E_{c.m.}+Q$ (MeV)	Average total photon energy T_γ (MeV)
$Nd^{142}(C^{12}, 3n)Dy^{151}$	
9.8	4.8
23.1	14.9
$Nd^{142}(C^{12}, 4n)Dy^{150}$	
15.6	7.5
27.9	17.4
35.8	22.8
$Ce^{140}(O^{16}, 5n)Dy^{151}$	
16.0	5.0
26.1	13.1
35.1	19.0
$Nd^{142}(C^{12}, 5n)Dy^{149}$	
17.5	7.4
25.4	13.5
33.4	19.7
43.6	26.1
53.8	31.3
$Nd^{144}(C^{12}, 5n)Dy^{151}$	
16.1	5.0
21.6	9.4
31.4	16.5
$Nd^{148}(C^{12}, 5n)Dy^{155}$	
10.1	2.7
19.9	8.6
31.0	16.2
36.2	20.7
$Nd^{150}(C^{12}, 5n)Dy^{157}$	
26.3	13.0
35.4	19.0
$Ce^{140}(O^{16}, 6n)Dy^{150}$	
18.6	5.3
27.6	11.5
36.7	17.1
45.0	24.7
52.9	30.6
$Nd^{141}(C^{12}, 6n)Dy^{150}$	
23.9	8.1
29.1	13.1
40.1	19.5
50.5	26.7
$Ce^{140}(O^{16}, 7n)Dy^{149}$	
17.2	−0.6
26.3	7.3
34.6	13.7
42.5	19.5
63.9	31.6
$Nd^{144}(C^{12}, 7n)Dy^{149}$	
13.5	−0.6
18.7	3.5
29.7	10.4
40.1	18.2
$Nd^{150}(C^{12}, 7n)Dy^{155}$	
45.6	19.4
$Gd^{154}(He^4, 7n)Dy^{151}$	
19.0	3.8
23.8	7.4
28.7	9.2
33.6	10.3
$Gd^{154}(He^4, 8n)Dy^{150}$	
26.1	7.6
31.0	9.7

[a] T_γ was calculated from Q values in Ref. 12, using the relationship $T_\gamma = E_{c.m.}+Q-T_n$.

[b] Measured values of T_n were taken from Refs. 2 and 6 and from this work.

reactions for which less extensive cross-section data are available.

In Table I, we give average angles and energies obtained with the assumption of isotropic neutron emission. (This assumption has been tested in Refs. 4–6.) The experiments were performed at the Yale Hilac by the same methods described in Ref. 2. The assay of Dy^{155} and Dy^{157} was performed by observation of the γ rays of 0.23 and 0.33 MeV. For angular distribution measurements, a NaI crystal 3×3 in. was employed, and for cross-section measurements, a Li-drifted Ge detector of 6 cm^3 was used. The cross-section data are given in Table II.

In Figs. 2–4 we show T_γ measurements for reactions in which three to eight neutrons are emitted. The data are from Refs. 2 and 6, and from this work. All values of T_γ have been obtained from Q values from Ref. 12. Therefore, some small differences may be noted from the values originally reported (originally Q values were

[12] V. Viola and G. T. Seaborg, J. Inorg. Nucl. Chem. **28**, 697 (1966).

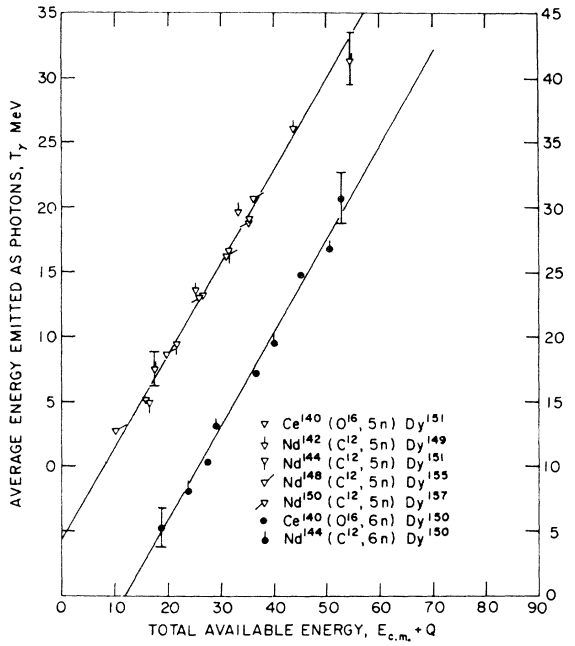

FIG. 3. Average total photon energy $T\gamma$ versus total available energy (in MeV) for (HI, $5n$) and (HI, $6n$) reactions.

obtained from Seeger's masses[13]). The whole collection of T_γ data is given in Table III.

The two most striking features of these figures are as follows: (a) A linear relationship between T_γ and $E_{c.m.}+Q$ provides a close fit to the data for each reaction. (b) The values of T_γ as a function of $E_{c.m.}+Q$ seem to depend only on the number of emitted neutrons. There is no apparent dependence on the target-projectile combination. We will take these observations seriously and assume that T_γ is given by a linear relationship

$$T_\gamma = a + b(E_{c.m.}+Q), \tag{9}$$

where the constants a and b depend only on x.

TABLE IV. Average angular momenta at peak cross section

Reaction	$(E_{c.m.}+Q)_{peak}$	$\langle J\rangle_{peak}$
$Ce^{140}(O^{16}, 5n)Dy^{150}$	27.4	37.4
$Nd^{142}(C^{12}, 5n)Dy^{149}$	28.1	35.2
$Nd^{144}(C^{12}, 5n)Dy^{151}$	26.1	32.8
$Nd^{148}(C^{12}, 5n)Dy^{155}$	23.5	28.5
$Nd^{150}(C^{12}, 5n)Dy^{157}$	23.4	26.2
$Ce^{140}(O^{16}, 6n)Dy^{150}$	35.8	45.2
$Nd^{144}(C^{12}, 6n)Dy^{150}$	33.7	39.0
$Ce^{140}(O^{16}, 7n)Dy^{149}$	39.5	51.2
$Nd^{144}(C^{12}, 7n)Dy^{149}$	≈37.0	≈45.0
$Nd^{150}(C^{12}, 7n)Dy^{155}$	32.2	38.3
$Gd^{154}(He^4, 7n)Dy^{151}$	29.4	25.2

[13] P. A. Seeger, Nucl. Phys. **25**, 1 (1961).

As stated previously, one expects that the total energy emitted as photons will depend on the angular momentum distribution of the excited nuclei. If this is true, how can we obtain feature (b) above? We must remember two aspects of reactions between complex nuclei and the decay of the compound nuclei that are formed: (1) One expects that "spin fractionation" will have a major effect on the relative cross sections for each (HI, xn) reaction. In other words, the division of reaction probability between the emission of x and $x-1$ neutrons will definitely depend on the initial distribution of angular momentum in the compound nuclei. This spin fractionation will work in the direction

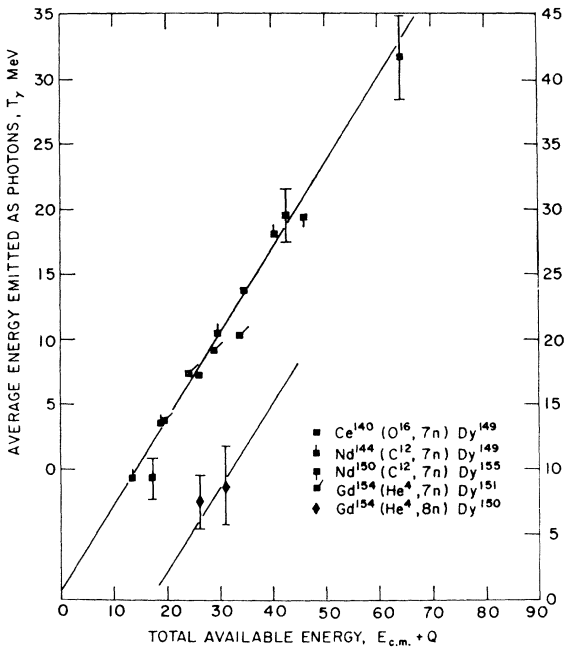

FIG. 4. Average total photon energy $T\gamma$ versus total available energy (in MeV) for (HI, $7n$) and (HI, $8n$) reactions.

of reducing differences between initial angular momentum distributions and those appropriate to particular (HI, xn) reactions. (2) The differences in average initial angular momentum (for any specific number of emitted neutrons) are usually not very great, even though the experimenter may make a special effort to select reactions to emphasize these differences.

We can get a feeling for these differences by making some simple estimates of the average initial angular momenta of the compound nuclei. The simplest approximation is provided by the sharp cutoff approximation

$$\langle J\rangle = (8\mu)^{1/2}R(E_{c.m.}-V)^{1/2}/3\hbar, \tag{10}$$

where μ is the reduced mass, R is the sum of the radii (radius parameter 1.5 F), and V is the Coulomb barrier. These values of $\langle J\rangle$ are calculated with the assumption that all reactions lead to compound-nucleus formation. It is known that breakup reactions do occur with

TABLE V. Evaluation of $\langle T_\gamma \rangle_x$ and $\langle T_n \rangle_x$ from various fits to T_γ.

Reaction	$\langle T_\gamma \rangle_x$	$\langle T_n \rangle_x$	$-a$	b	Source of a and b
$Ce^{140}(O^{16}, 5n)Dy^{151}$	14.8	14.3	6.53	0.734	This reaction only
	15.0	14.1	6.09	0.724	Smooth curve
$Nd^{142}(C^{12}, 5n)Dy^{149}$	17.5	14.0	3.38	0.662	This reaction only
	16.7	14.8	6.09	0.724	Smooth curve
$Nd^{144}(C^{12}, 5n)Dy^{151}$	13.0	13.6	6.94	0.748	This reaction only
	13.2	13.4	6.09	0.724	Smooth curve
$Ce^{140}(O^{16}, 6n)Dy^{150}$	18.8	18.6	8.94	0.741	This reaction only
	18.4	19.1	7.87	0.701	Smooth curve
$Nd^{144}(C^{12}, 6n)Dy^{150}$	16.8	19.0	7.49	0.678	This reaction only
	17.2	18.6	7.87	0.701	Smooth curve
$Ce^{140}(O^{16}, 7n)Dy^{149}$	17.9	24.3	10.92	0.683	This reaction only
	18.1	24.1	9.36	0.650	All (HI, $7n$) data
	18.2	24.0	9.32	0.653	All (HI, $7n$) data, negative $T_\gamma \equiv 0$
	18.6	23.5	9.87	0.676	(HI, $7n$) data excluding two points
	18.6	23.6	9.41	0.663	(HI, $7n$) data excluding two points, negative $T_\gamma \equiv 0$
	18.9	23.3	9.65	0.677	Smooth curve
$Nd^{144}(C^{12}, 7n)Dy^{149}$	16.9	21.6	9.86	0.695	This reaction only
	15.7	22.8	9.36	0.650	All (HI, $7n$) data
	15.8	22.7	9.32	0.653	All (HI, $7n$) data, negative $T_\gamma \equiv 0$
	16.2	22.3	9.87	0.676	(HI, $7n$) data excluding two points
	16.1	22.4	9.41	0.663	(HI, $7n$) data excluding two points, negative $T_\gamma \equiv 0$
	16.4	22.1	9.65	0.677	Smooth curve

significant cross sections, and there is evidence that these reactions are most probable for large values of the orbital angular momentum.[14] Thus we can infer that there are systematic overestimates in $\langle J \rangle$ which increase as $\langle J \rangle$ increases.

In Table IV we give $\langle J \rangle$ (calculated in this simple way) for compound nuclei formed at the energy of maximum cross section in reactions for which 5, 6, or 7 neutrons were emitted.[15] From these values one can see the maximum span of the average angular momenta involved in the reactions for which we have T_γ data. We conclude from Table IV and Figs. 3 and 4 either that a and b of Eq. (9) do not depend on the initial value of $\langle J \rangle$, or that the reaction mechanism reduces the effect below the detection limit.

In Fig. 5 we show values of the slopes b and intercepts a obtained from Figs. 2–4. These values were obtained by least-squares fits for one scheme of weighting of the data points. Slightly different values result for various schemes of weighting as shown in Table V. These will be discussed in the context of estimation of errors (the Appendix). The trend of results for a and b is very regular and allows linear extrapolation for reactions (HI, $8n$, $9n$, $10n$, and $11n$). Note that negative values of T_γ are implied by Eq. (9) for energies near the threshold for reaction. The crossover point where $T_\gamma = 0$ is also shown in Fig. 5. Clearly, these negative values of T_γ are meaningless, and their effect must be removed from the analysis. This removal is automatically performed by the cross sections which become very small in this region. In other words, there is negligible contribution to the integral in Eq. (6) from the energy region of $E_{\text{c.m.}} + Q < -a/b$.

Values of $\langle T_\gamma \rangle_x$ can be obtained by substitution of Eq. (9) into Eq. (6):

$$\langle T_\gamma \rangle_x = a + b(\langle E \rangle_x + Q), \tag{11}$$

and, similarly, values of $\langle T_n \rangle_x$ can be obtained from

$$\langle T_n \rangle_x + \langle T_\gamma \rangle_x = \langle E \rangle_x + Q. \tag{12}$$

[14] R. Kaufmann and R. Wolfgang, Phys. Rev. **121**, 192 (1961); **121**, 206 (1961).

[15] F. Lanzafame and J. M. Alexander (unpublished).

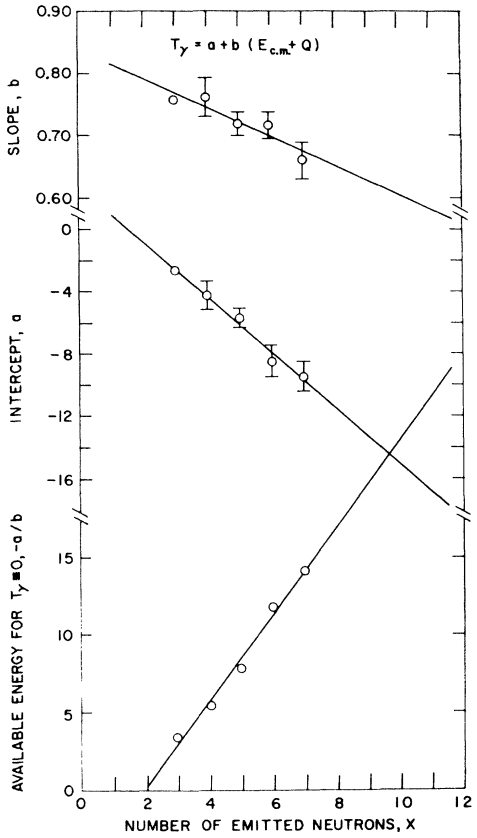

FIG. 5. Slope a, intercept b, and $-a/b$ for linear least-squares fits to the data in Figs. 2, 3, and 4.

In Figs. 6 and 7 and in Table VI we list these quantities and show their dependence on $\langle J\rangle$ from Eq. (10). Systematic overestimates of $\langle J\rangle$ will not provide any problems in the interpretation of $\langle T_n\rangle_x$ if the angular momentum dependence of $\langle T_n\rangle$ is small. We have determined that the slope $d\langle T_n\rangle/d\langle J\rangle$ is only 0.12 ± 0.03 MeV (as described below), which is the main feature that we were seeking, and which allows us to obtain values of $\langle\epsilon_1\rangle$ from the energy displacements between different reactions [Eq. (8) and Fig. 6)]. Our estimate is that the values of $\langle\epsilon_1\rangle$ obtained from Fig. 6 are uncertain by only about 0.5 MeV. In Fig. 6 we show 19 data points that are not given in Table VI. These data cover a wide span of $\langle J\rangle$ and, therefore, are very helpful in fixing the slope $d\langle T_n\rangle/d\langle J\rangle$. The values were obtained (as described below) in a much less precise way than those in Table VI; therefore, they are denoted in Fig. 6 by symbols (numerals) which make them easily distinguishable.

For many (HI, xn) reactions, the measurements are not extensive enough to permit determination of $\langle E\rangle$ by integration of Eq. (1). However, it is often possible to define the energy E_p corresponding to the maximum (or peak) cross section. In Ref. 14 we have collected data of this type and have shown empirically that there is a simple relationship between E_p and $\langle E\rangle$. This relationship is

$$\langle E\rangle/E_p = 1.087\pm 0.019 - (0.033\pm 0.028)x. \quad (13)$$

From this relationship we have estimated $\langle E\rangle$ from several reactions induced by He^4, C^{12}, Ne^{22}, and Ar^{40}. Then we used Eqs. (11) and (12) and Fig. 5 to obtain $\langle T_n\rangle$ and $\langle T_\gamma\rangle$. The values are shown in Figs. 6 and 7. For reactions involving emission of 4–8 neutrons, we made least-squares linear fits to $\langle T_n\rangle$ versus $\langle J\rangle$ and determined the average slope $d\langle T_n\rangle/d\langle J\rangle$ to be 0.12 ± 0.03 MeV/$\hbar$. Lines with this slope are drawn through the points in Fig. 6. The arrows indicate the displacements $\langle\epsilon_1\rangle$ between the lines.

The meaning of these values of $\langle\epsilon_1\rangle$ in terms of evaporation theory is shown in Fig. 8. The simple form of the theory has been used to draw the smooth curves for different a parameters. One should not take the exact magnitude of a shown here too seriously, because spin restrictions must play some role.[7] The significant result is that these values of $\langle\epsilon_1\rangle$ will delimit the value of a to about $\pm 25\%$ for the span of excitation energies 45–155 MeV.

TABLE VI. Values of $\langle T_\gamma\rangle_x$ and $\langle T_n\rangle_x$.

Reaction	$\langle T_\gamma\rangle_x$	$\langle T_n\rangle_x$	$-a$	b
$Nd^{142}(C^{12}, 3n)Dy^{151}$	12.3	6.9	2.53	0.772
$Nd^{142}(C^{12}, 4n)Dy^{150}$	15.2	10.9	4.31	0.748
$Nd^{142}(C^{12}, 5n)Dy^{149}$	16.7	14.8	6.09	0.724
$Pr^{141}(N^{14}, 4n)Dy^{151}$	11.3	9.6	4.31	0.748
$Pr^{141}(N^{14}, 5n)Dy^{150}$	15.4	14.3	6.09	0.724
$Pr^{141}(N^{14}, 6n)Dy^{149}$	16.8	18.4	7.87	0.701
$Nd^{144}(C^{12}, 5n)Dy^{151}$	13.2	13.4	6.09	0.724
$Nd^{144}(C^{12}, 6n)Dy^{150}$	17.2	18.6	7.87	0.701
$Pr^{141}(N^{15}, 6n)Dy^{150}$	17.1	18.5	7.87	0.701
$Pr^{141}(N^{15}, 7n)Dy^{149}$	18.0	22.8	9.65	0.677
$Ce^{140}(O^{16}, 5n)Dy^{151}$	15.0	14.1	6.09	0.724
$Ce^{140}(O^{16}, 6n)Dy^{150}$	18.4	19.1	7.87	0.701
$Ce^{140}(O^{16}, 7n)Dy^{149}$	18.9	23.3	9.65	0.677
$Ba^{136}(Ne^{20}, 5n)Dy^{151}$	16.0	14.5	6.09	0.724
$Ba^{136}(Ne^{20}, 6n)Dy^{150}$	18.8	19.2	7.87	0.701
$Ba^{136}(Ne^{20}, 7n)Dy^{149}$	18.9	23.3	9.65	0.677
$Ba^{137}(Ne^{20}, 6n)Dy^{151}$	19.1	19.4	7.87	0.701
$Ba^{137}(Ne^{20}, 7n)Dy^{150}$	20.7	24.1	9.65	0.677
$Ba^{137}(Ne^{20}, 8n)Dy^{149}$	20.9	28.5	11.43	0.654
$Ce^{140}(O^{18}, 7n)Dy^{151}$	19.2	23.4	9.65	0.677
$La^{139}(F^{19}, 7n)Dy^{151}$	18.7	23.2	9.65	0.677
$La^{139}(F^{19}, 8n)Dy^{150}$	20.7	28.4	11.43	0.654
$La^{139}(F^{19}, 9n)Dy^{149}$	20.3	32.9	13.21	0.630
$Ba^{138}(Ne^{20}, 7n)Dy^{151}$	18.6	23.1	9.65	0.677
$Ba^{138}(Ne^{20}, 8n)Dy^{150}$	21.0	28.6	11.43	0.654
$Ba^{138}(Ne^{20}, 9n)Dy^{149}$	20.3	32.9	13.21	0.630
$Ba^{137}(Ne^{22}, 8n)Dy^{151}$	22.3	29.3	11.43	0.654
$Ba^{137}(Ne^{22}, 9n)Dy^{151}$	23.5	34.8	13.21	0.630
$Ba^{138}(Ne^{22}, 9n)Dy^{151}$	21.7	33.7	13.21	0.630

It is interesting that the values of $\langle T_n \rangle$ shown in Fig. 6 are about 25% greater than the sums obtained from Fig. 8. For example, $\langle T_n \rangle \approx 19$ MeV, while the sum of the $\langle \epsilon_1 \rangle$ value for first of 6, plus that for the first of 5, etc., is about 15 MeV. We believe that this is a real effect which reflects spin restrictions on subsequent neutron emissions. With each subsequent neutron emission in an evaporation chain, the spin-dependent level density exerts more pull toward larger angular momentum and energy removal. In evaporation calcu-

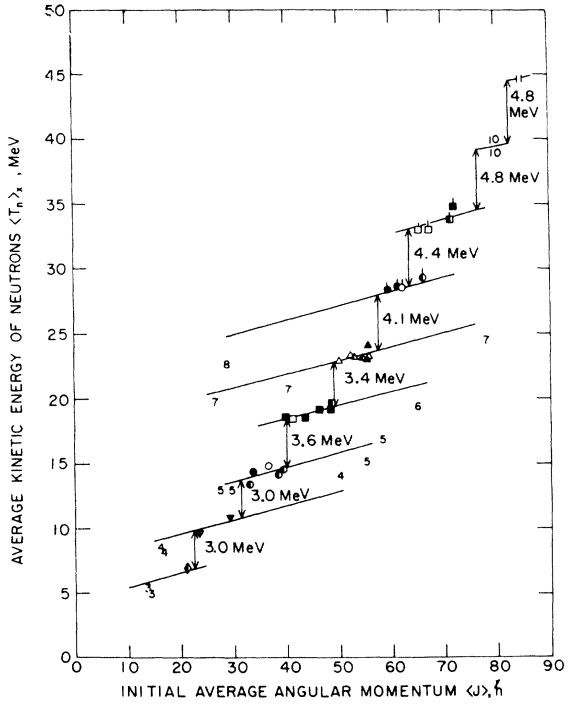

FIG. 6. Average total neutron energy $\langle T_n \rangle_x$ as a function of the average initial angular momentum $\langle J \rangle$. Symbols are the same as in Fig. 1, except that small numerals indicate $\langle T_n \rangle$ values estimated from E_p (see text). The average energy of the first emitted neutron $\langle \epsilon_1 \rangle$ is indicated by displacement.

lations, the later emissions should be influenced by spin cutoff parameters much more than the first neutron emissions. This, of course, is the basis for our desire to obtain $\langle \epsilon_1 \rangle$ as a focus on the a parameter.

Let us now turn to the interpretation of Fig. 7. As we pointed out earlier, the major feature of the statistical model which affects photon emission is the magnitude of the yrast levels E_J.[9] A rough estimate of the relationship between $\langle T_\gamma \rangle$ and E_J is that

$$E_J = \langle T_\gamma \rangle - B_n, \tag{14}$$

where the $\langle J \rangle$ value appropriate to $\langle T_\gamma \rangle$ is the initial $\langle J \rangle$ less that removed by the neutrons ($\sum \Delta J$).[7,8] The straight lines shown on Fig. 7 show subtractions of B_n and $\sum \Delta J_i$ from $\langle T_\gamma \rangle_x$. It is clear from the trend of T_γ

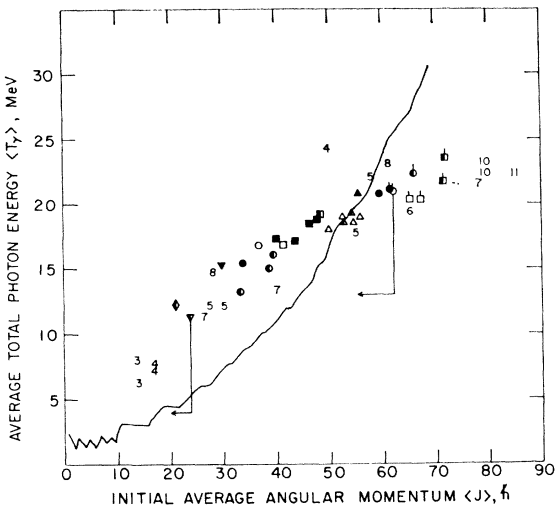

FIG. 7. Average total photon energy $\langle T_\gamma \rangle_x$ as a function of the average initial angular momentun $\langle J \rangle$. Symbols are as in Figs. 1 and 6. Vertical arrows show subtraction of the separation energy of the neutron; horizontal arrows show subtraction of $1\hbar$ unit per emitted neutron. The yrast levels shown were calculated by Grover using a shell model (Ref. 10).

values that yrast levels estimated as described differ significantly from those calculated by Grover.[11] We must, however, include another effect in the estimate of E_J from the experiments. This is the calculation of the intial angular momentum distribution. As mentioned previously, we have assumed that all reactions lead to compound-nucleus formation, even though it is probable that "breakup" reactions occur mainly at large impact parameters, thereby robbing population from the states of high J.[14] We can obtain an upper limit for this effect from the f_n measurements shown in Fig. 2 of Ref. 3. We assume, in order to obtain this limit, that all reactions other than (HI, xn) reactions are breakup reactions proceeding through the states of highest l (or J). The

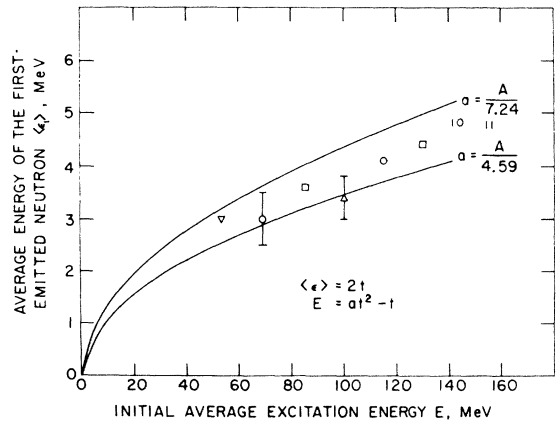

FIG. 8. Average energy of the first emitted neutron as a function of excitation energy. Lines show the predictions of the simplest form of the statistical model. The symbols are the same as those in Fig. 6.

initial values of $\langle J \rangle$ will be decreased from those shown by the factor $(f_n)^{1/2}$, which varies from 0.9 to 0.6 as we move from low to high J. In particular, the tip of the arrow at $\langle J \rangle = 20$ would be moved to $\langle J \rangle = 18$, and the arrow at $\langle J \rangle = 55$ would be moved to $\langle J \rangle = 35$. With these corrections, the observed values of $\langle T_\gamma \rangle_x$ are consistent with the shell-model calculations of the yrast levels.[11] Of course this delimitation of E_J can be improved markedly by a more complete analysis and by measurements of cross sections for compound-nucleus formation.[16]

ACKNOWLEDGMENTS

We thank D. Weiner and G. Waldron for help in carrying out experiments. A discussion with Professor R. Vandenbosch stimulated our consideration of this analysis. Dr. J. Gilat, Dr. A Pape, and Dr. F. Lanzafame have been kind enough to make their results available before publication.

APPENDIX: SYSTEMATIC AND RANDOM ERRORS

It is certainly an ambitious task to try to determine neutron energies to ± 0.5 MeV from reaction studies involving beam energies from 60 to 220 MeV. The use of Eqs. (4)–(8) requires taking a difference between two rather large numbers, a procedure which is always hazardous. However, one must remember that many of the sources of error in either $\langle E \rangle_x$ or $\langle T_n \rangle_x$ are systematic and will tend to cancel when we take the differences. Uncertainty in the absolute velocity of the beam from the accelerator mainly affects this analysis by day-to-day variations, and this effect is averaged out by repeated experiments. Errors in the values of Q only enter through the separation energy of the first neutron, and these errors will probably alternate in magnitude as we compare (HI, $9n$) to (HI, $8n$), then (HI, $8n$) to (HI, $7n$), etc. Errors in absolute values of the cross sections from branching ratios, counting efficiencies, target thicknesses, etc., are not important. Only the shapes of the excitation functions are important.

The systematics obtained for T_γ as a function of $E_{\text{c.m.}}+Q$ are the key to this analysis. Let us look at these assumptions in some detail. We have assumed that T_γ is dependent only on x, not on J. One would expect that if this assumption is incorrect, then the slopes $d\langle T_n \rangle_x / d\langle J \rangle$ would be reduced from that shown in Fig. 6. The slopes in Fig. 6 are only 0.12 MeV/$\hbar$, so that even if this is reduced to zero, the values $\langle \epsilon_1 \rangle$ would be increased by only ≈ 0.5 MeV.

The relationship that we use for T_γ [$T_\gamma = a + b(E_{\text{c.m.}}+Q)$] for $E_{\text{c.m.}}+Q > -a/b$ and $T_\gamma = 0$ for $E_{\text{c.m.}}+Q < -a/b$ has the disadvantage that it leads to a discontinuity in T_γ near threshold. On physical grounds, we do not expect such a discontinuity. The error associated with this effect is minimized by the small cross sections in this energy region and is also washed out by subtraction of $\langle T_n \rangle_{x-1}$ from $\langle T_n \rangle_x$. A similar error may occur at high values of $E_{\text{c.m.}}+Q$ as indicated by the tendency of measured values of T_γ to fall below the least-squares line. This tendency is not outside the experimental uncertainties in T_γ. Of course, systematic errors in T_γ from corrections for scattering or angular resolution are all very similar and will be largely canceled by subtraction.

In Table V we give a series of values of $\langle T_\gamma \rangle$ and $\langle T_n \rangle$ obtained from different T_γ functions. The different T_γ functions (characterized by a and b) were obtained by least-squares fits to the data with different values of $\langle T_n \rangle$; the average deviation from the smooth curve values is ± 0.5 MeV. We feel that the best fit is probably that obtained by giving low weight to the highest-energy points (for the $5n$ and $7n$ reactions only). These points may well reflect a deviation from linearity, and, since we are forcing a linear fit, they may exert an undue influence on the slope of the line.

A comparison of Figs. 1 and 6 shows that the transformation from $\langle E \rangle_x$ to $\langle T_n \rangle_x$ has had two effects. First, the slope with $\langle J \rangle$ has been reduced by about fourfold. Second, much of the scatter has been removed. One might say that this is the result of using smoothed functions for T_γ and, therefore, T_n. We think that this is a real physical effect and not just a result of smoothing. The values of $\langle T_\gamma \rangle_x$ are heavily weighted toward large values of $E_{\text{c.m.}}+Q$; correspondingly, the values of $\langle T_n \rangle_x$ are weighted toward lower energies. It is quite likely that different reactions with different projectiles and targets have certain irregularities which derive from the influence of breakup reactions on cross-sections and J distributions. These irregularities would be expected to be more prominent at the higher energies and, therefore, to carry the scatter in $\langle E \rangle_x$ mainly into $\langle T_\gamma \rangle_x$. Comparison of Figs. 1, 6, and 7 shows this to be the case. Figure 7 allows us to test our assumption that ${}_J\langle T_\gamma \rangle_x = {}_{J-\Delta J}\langle T_\gamma \rangle_{x-1}$ to within the scatter of the points. It appears that a shift in ΔJ of 2–$4\hbar$ is indicated as in Ref. 3. However, as mentioned earlier, it is likely that much of this shift is due to the increasing effect of breakup reactions as energy is increased.

To summarize, it is not possible to carry through a precise error evaluation for this analysis, but the scatter of the values of $\langle T_n \rangle_x$ in Tables V and VI and in Fig. 6 indicates that the errors in the $\langle \epsilon_1 \rangle$ values are about ± 0.5 MeV as shown in Fig. 8.

[16] L. Kowalski, J. C. Jodogne, and J. M. Miller, Phys. Rev. **169**, 894 (1968); J. B. Natowitz, in Proceedings of the American Chemical Society, Minneapolis, Minn., 1969 (unpublished).